iJRASET
International Journal For Research in
Applied Science and Engineering Technology

INTERNATIONAL JOURNAL
FOR RESEARCH
IN APPLIED SCIENCE & ENGINEERING TECHNOLOGY

Volume: 6 **Issue:** IV **Month of publication:** April 2018

DOI: http://doi.org/10.22214/ijraset.2018.4688

www.ijraset.com

Call: ✆08813907089 | E-mail ID: ijraset@gmail.com

International Journal for Research in Applied Science & Engineering Technology (IJRASET)
ISSN: 2321-9653; IC Value: 45.98; SJ Impact Factor: 6.887
Volume 6 Issue IV, April 2018- Available at www.ijraset.com

Liquid Phase Benzylation of O-Xylene on Nano Mesoporous Lanthanum Aluminates

Marymol Moothedan[1], K. B. Sherly[2]
[1, 2] Regional Research Centre of M.G. University, Mar Athanasius College, Kothamangalam, Kerala, India, 686666

Abstract: Nano lanthanum aluminates synthesized by sol-gel method were used for the liquid phase benzylation of o-xylene (o-Xyl) with benzyl chloride (BC) in a batch reactor at atmospheric pressure. Lanthanum aluminates were characterized in depth by Differential thermo gravimetric analysis (DTG), Differential scanning calorimetric analysis (DSC), X-ray diffraction (XRD), Fourier transform infrared spectroscopy (FTIR), N_2 sorpometry, transmission electron microscopy (TEM), temperature-programmed desorption using CO_2/NH_3 (CO_2-TPD/NH_3-TPD) and temperature-programmed reduction using H_2 (H_2-TPR) in order to relate its performances to the chemical and textural characteristics. Nano $La_{10}Al_4O_{21}$ was detected for lower aluminum precursor concentration and stable nano mesoporous $LaAlO_3$ becomes the major phase as the concentration increases. The band gap of $LaAlO_3$ and $La_{10}Al_4O_{21}$ was estimated from ultraviolet-visible (UV-Vis) spectrophotometry. Ac conductivity and dielectric measurement of lanthanum aluminates were also performed. The effect of catalyst concentration, reaction temperature, reaction time and o-Xyl/BC molar ratio on benzylation of o-Xyl was studied over stable nano mesoporous $LaAlO_3$ and was extended to nano $La_{10}Al_4O_{21}$ at the optimized conditions. $LaAlO_3$ showed 92% and $La_{10}Al_4O_{21}$ showed 51% BC conversion at the following reaction conditions (catalyst to BC (w/w) = 0.1, o-Xyl/BC molar ratio =1:1, 433K, 2h, 1 atm). The acidity and mesoporous structure of $LaAlO_3$ appeared to be responsible for its good performance. Increase in catalyst concentration, reaction temperature and reaction time enhances the conversion of BC, whereas it decreases with the increase in o-Xyl/BC molar ratio. The Friedel-Crafts (FC) benzylation reaction mechanism involves the formation of an electrophile ($C_6H_5CH_2^+$) over an acidic lanthanum aluminate catalyst which attacks the O-Xyl ring resulting in the formation of 3,4 –dimethyl diphenyl methane.

***Keywords**: Benzylation; Lanthanum aluminates; $La_{10}Al_4O_{21}$;; Sol gel; Mesoporous;*

I. INTRODUCTION

Rare earth aluminates have attracted keen interest over the years owing to their unique physical and chemical properties [1]. Among them lanthanum aluminates have attracted wide-spread attention in different frontier areas of research due to their outstanding potential in superconductors [2], radiation dosimetry [3], memory devices [4], semiconductor [5], thermal barrier coating [6] and heterogeneous catalysis [7].

In addition, when a mixed metal oxide attains mesoporosity with appreciable good surface area, it can play key role in many industrial applications [8]. Even though large varieties of mesoporous materials have been studied intensively, little attention have been paid to the synthesis of mesoporous mixed metal oxides and their application potentials. Lanthanum aluminate is generally synthesized via solid state reactions [9], co-precipitation [10] or polymer complexing plus combustion method [11]. But the environmentally benign citrate-sol gel method has been rarely employed.

The construction of C-C bond by FC benzylation has revolutionized organic synthesis and chemical manufacturing [12]. The product, dimethyldiphenylmethanes (DMDPM) have many useful applications [13, 14]. To the best of our knowledge FC benzylation by nano mesoporous lanthanum aluminates has not reported so far. FC benzylation in the presence of homogeneous and heterogeneous catalysts, although giving better yields in industrial scale; these catalysts, however have several drawbacks such as toxicity, corrosiveness, less activity, moisture sensitivity etc [13, 15]. Thus we need a non-corrosive, non toxic, active heterogeneous solid catalyst, which can be synthesized in a convenient, cost-effective and environmentally friendly route. In this context, successful synthesis and utilization of mesoporous lanthanum aluminates is very much important.

II. EXPERIMENTAL

A. Catalyst preparation

All chemicals were analytical grade and were used without further purification. Lanthanum aluminates were synthesized by the modified citrate sol-gel method [16]. Citric acid was added to the premixed lanthanum and aluminum nitrate solution while stirring, such that molar ratio of acid/La+Al = 2. The solution was heated in a water bath until a viscous gel was obtained. The gel was dried at 110°C overnight to form a spongy material. The dried gel was calcined at 800°C for 6 hrs.

B. Catalyst Characterization

The thermal behavior of the dried gel was examined by DTG/DSC analysis using Perkin Elmer STA 6000 thermo gravimetric apparatus. The phases were identified by means of XRD with a RIGAKU D/MAX-C diffractometer using Cu Kα radiation (λ = 1.5405Á) at a scanning rate of $5^o\ s^{-1}$. Surface morphology was evaluated by TEM (HR-TEM-JEOL, JEM-2100). FT-IR studies were done in KBr medium using Thermo Nicolet Avatar 370 model FT-IR spectrophotometer. UV-Vis diffuse reflectance spectra were recorded over a wavelength range between 200 to 2000 nm using a Varian, Cary 5000 spectrometer. Surface properties were determined using Micromeritics Gemini VII surface area and porosity analyzer by N_2 adsorption at 77K, according to the standard Brunauer –Emmer-Teller (BET) method. The Lewis basicity and acidity were studied by CO_2-TPD, NH_3-TPD experiments using Micromeritics ChemiSorb 2750 pulse chemisorption apparatus. Reduction characteristics were analyzed by H_2-TPR analysis using the same Micromeritics chemisorption apparatus. Dielectric characterization was done by using Agilent 16451B Impedance analyzer in parallel mode at frequencies ranging from 40 Hz to 1 MHz.

C. Catalytic Activity

The catalytic activity of nano mesoporous lanthanum aluminates was tested for FC benzylation of o-Xyl with BC in solvent free liquid phase reaction. The benzylation was performed in liquid phase batch reactor consists of a round bottom flask with condenser, in a constant temperature oil bath with magnetic stirring. In typical run, appropriate amounts of o-Xyl and BC (1:1 and 5:1 molar ratio) was charged in the reactor along with 0.05 to 0.25 g catalyst. The reaction mixture was heated to 303 to 473 K under stirring for 30 to 190 min. Samples were withdrawn periodically and analyzed with a gas chromatograph (Perkin Elmer Clarus 650) fitted with a flame ionization detector and Elite 5 capillary column. Some selected runs were analyzed by GC-MS for product identification.

III. RESULTS AND DISCUSSION

A. Catalyst Characterization

1) Thermal analysis: Fig. 1 shows the results of thermal analysis of $LaAlO_3$ precursor prepared by citrate sol-gel method. The first weight loss of about 13%, at 100ºC in the DTG curve is due to dehydration. The endothermic peak around 550ºC in the DSC curve, accompanied by weight loss of about 16%, is due to the degradation of the residual citric acid and the elimination of residual CO_3^{2-} and NO_3^- ions [17]. The weight loss of about 5% at 780ºC is associated with further oxidation of the sample.

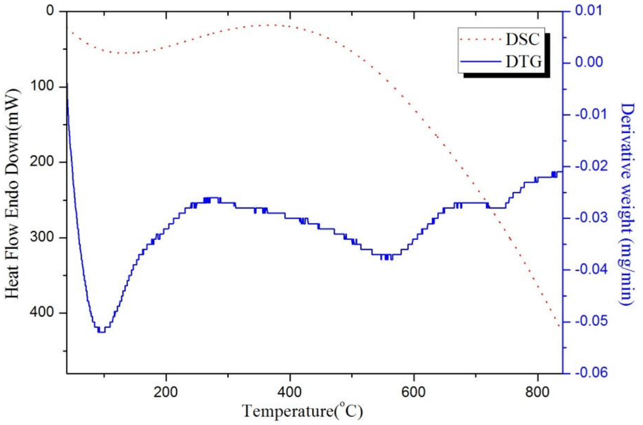

Fig. 1 Differential thermo gravimetric analysis and differential scanning calorimetric analysis of $LaAlO_3$ precursor

2) Formation of $LaAlO_3$: Fig. 2 shows XRD patterns of samples prepared by citrate sol gel method and calcined at 800ºC for 6 hrs. Secondary phase of orthorhombic $La_{10}Al_4O_{21}$ were detected (JCPDS 39-0009) for the sample prepared by using 0.030M $Al(NO_3)_3$. $LaAlO_3$ phase with rhombohedral structure (JCPDS 31-0022) begins to appear as the concentration of $Al(NO_3)_3$ increases and becomes the major phase as the concentration reaches to 0.05M. Formation of La_2CO_3 and $La(OH)_3$ were also identified at lower $Al(NO_3)_3$ concentrations (0.005M-0.020M).

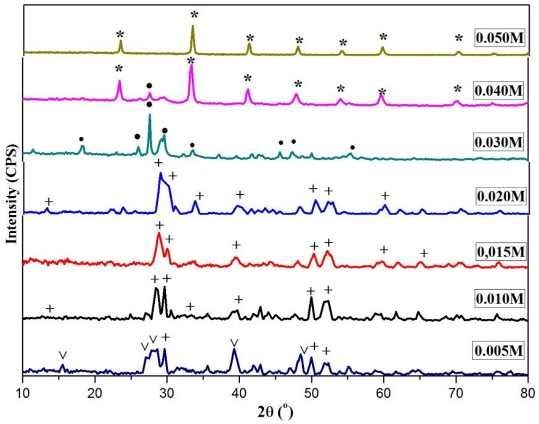

Fig. 2 XRD patterns of samples prepared by citrate sol-gel method using varying concentration of $Al(NO_3)_3$ calcined at 800°C for 6 hrs(* - $LaAlO_3$, •- $La_{10}Al_4O_{21}$, +- La_2CO_3, v- $La(OH)_3$)

3) FT-IR spectroscopy: Fig. 3 shows the FT-IR spectra of $LaAlO_3$ and $La_{10}Al_4O_{21}$. The broad absorption band at 3430 cm^{-1} is associated with the O-H stretching vibrations and the bands at 1200-1000 cm^{-1} were assigned to O-H bending vibrations of molecular water [18]. The bands around 880-440 cm^{-1} in the spectra were assigned to Al-O vibrational modes [19]. The peaks around 2349 cm^{-1} and 1617- 1493 cm^{-1} can be assigned to angular vibration modes and stretching modes of carbonate groups [20]. The results indicate the presence of immense amount of adsorbed water and CO_2 on $La_{10}Al_4O_{21}$ compared to $LaAlO_3$.

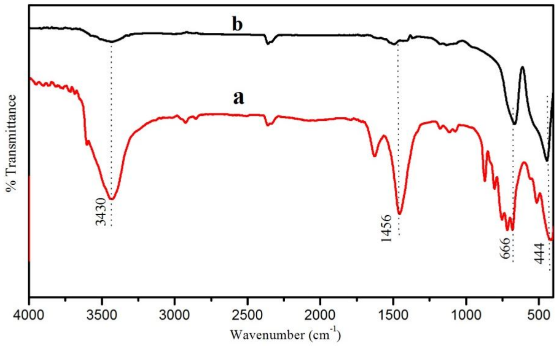

Fig. 3 FT-IR spectra of nano (a) $La_{10}Al_4O_{21}$ (b) $LaAlO_3$

4) Optical absorbance: UV-Vis absorption study was carried out in order to determine the band gap of nano lanthanum aluminates. The optical band gap was estimated by plotting $(\alpha h\upsilon)^2$ versus photon energy ($h\upsilon$), based on the relation $\alpha h\upsilon = A(h\upsilon - Eg)^{1/2}$,where α is the absorption coefficient, A is a constant, Eg is the band gap [21], Fig. 4. The higher optical band gap of orthorhombic $La_{10}Al_4O_{21}$ (5.2 eV) compared to rhombohedral $LaAlO_3$ (4.6 eV) may be due to difference in their lattice constants [22].

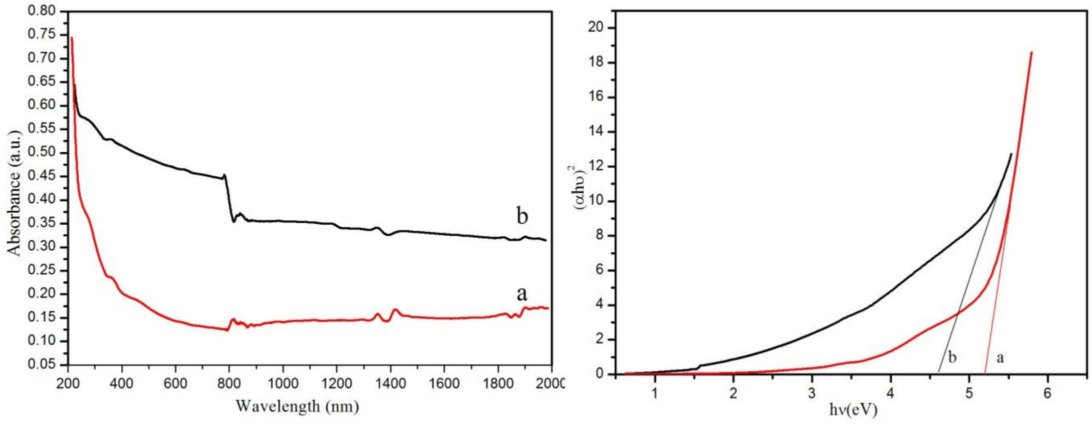

(i) (ii)

Fig. 4 (i) UV-Vis absorption spectra and (ii) Tauc plot of nano (a) $La_{10}Al_4O_{21}$ (b) $LaAlO_3$

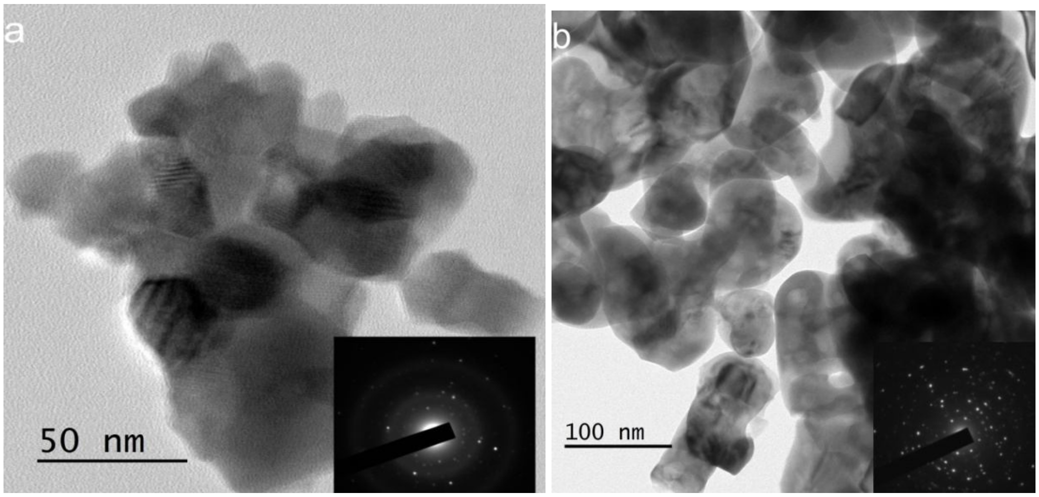

Fig. 5 TEM morphology of nano (a) $La_{10}Al_4O_{21}$ (b) $LaAlO_3$

5) Particle size and Morphology: The size and morphology of $La_{10}Al_4O_{21}$ and $LaAlO_3$ nano particles were shown in the Fig. 5 (a) & b. In contrast to $La_{10}Al_4O_{21}$ powder, $LaAlO_3$ powder has a rather regular shape and is weakly agglomerated. However, $La_{10}Al_4O_{21}$ has less particle size (35-40 nm) compared to $LaAlO_3$ (65-70 nm).

6) Surface area : The total surface area of lanthanum aluminate nanoparticles were obtained by Brunauer–Emmett–Teller (BET) method using N_2 adsorption-desorption isotherm data. All experimental parameters of BET surface area analysis were summarized in Table I. Nano $La_{10}Al_4O_{21}$ has large surface area with large pore diameter compared to nano $LaAlO_3$. Fig. 6 shows the BJH plots for N_2 adsorption-desorption isotherm and pore size distribution of lanthanum aluminate nano particles. Typical type V isotherm with H_3 type hysteresis loops at high P/P_0 value is observed for nano $LaAlO_3$, characteristics of large mesopores [23]. Hysteresis loop in nano $La_{10}Al_4O_{21}$ may due to tensile strength effect [24].

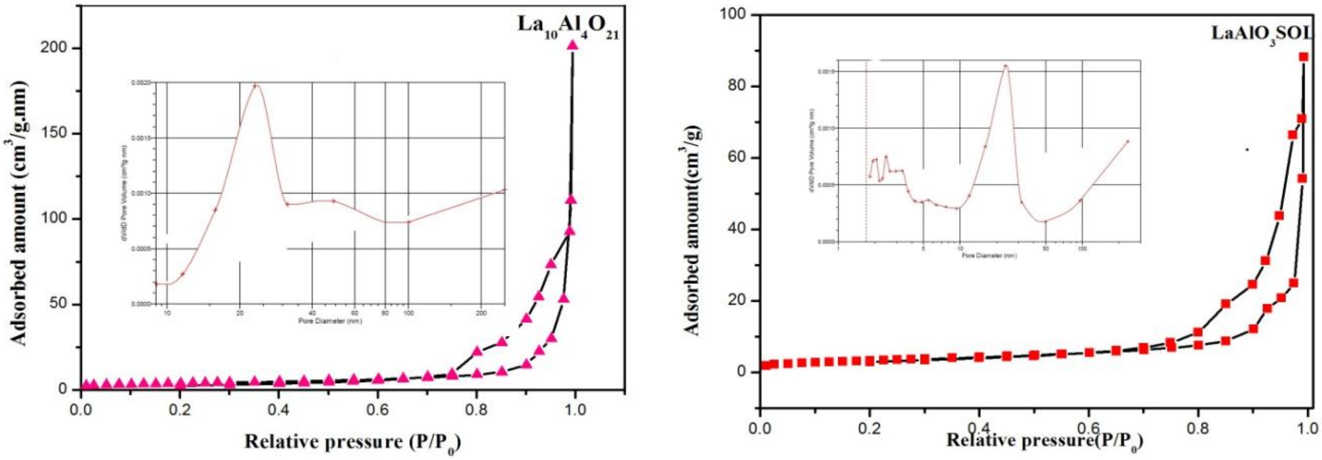

(a) (b)

Fig. 6 N_2 adsorption-desorption isotherm and pore size distribution of nano (a) $La_{10}Al_4O_{21}$ (b) $LaAlO_3$

Table I Experimental Parameters Of Bet Surface Area Analysis Of Nano Lanthanum Aluminates

Sample	BET Surface area (m^2/g)	BJH pore volume (cm^3/g)	BJH adsorption average pore diameter (nm)	BJH desorption average pore diameter (nm)
$La_{10}Al_4O_{21}$	13.4	0.31	82.2	100.8
$LaAlO_3$	12.4	0.31	48.7	28.2

Table Ii Lewis Sites Distribution In Nano Lanthanum Aluminate Evaluated On The Basis Of Co_2-Tpd/ Nh_3-Tpd

Sample	Basic sites ($\mu molg^{-1}$)				Acid sites ($\mu molg^{-1}$)			
	Weak	Strong	Very strong	Total	Weak	Strong	Very strong	Total
$La_{10}Al_4O_{21}$	13.9	61.4	120.9	196.2	41.7	600.08	290.11	931.9
$LaAlO_3$	58.3	-	-	58.3	57.8	83.3	900.2	1041.3

7) Surface acidity and basicity : For metal oxides, the metal ions are Lewis acid sites whereas the surface lattice oxygen are Lewis basic sites. CO_2-TPD, NH_3-TPD profiles of lanthanum aluminates is shown in the Fig. 7. From the figure it is clear that $LaAlO_3$ surface has higher no of Lewis acidic sites and less no of Lewis basic sites compared to $La_{10}Al_4O_{21}$. According to desorption temperature Lewis sites in lanthanum aluminates are categorized into weak (<200°C), strong (200-600°C) and very strong sites (>600°C) [25], Table. II. Lewis basic sites with weak strength mostly corresponds to OH^- groups on the catalyst surface, while those with strong and very strong strength are related to the oxygen of $M^{n+}O^{2-}$ ion pair and isolated O^{2-} anions [26]. Lewis acidity depends on the existence of exposed metal cations at the surface [27].

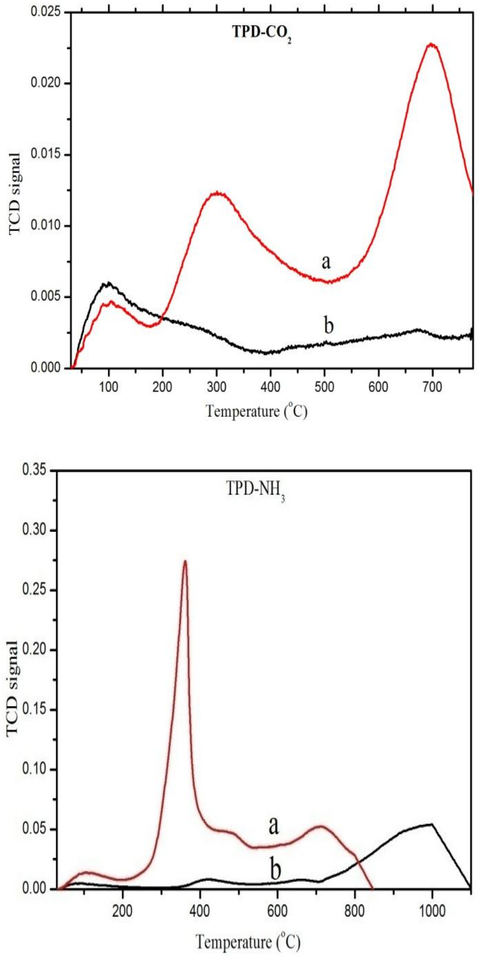

Fig. 7 CO_2-TPD, NH_3-TPD profile of nano (a) $La_{10}Al_4O_{21}$ (b) $LaAlO_3$

8) Reducibility: The H_2-TPR profiles of lanthanum aluminates are shown in the Fig. 8. In this figure H_2 consumption equates to oxidation of H_2 molecules by lanthanum aluminates. Thus we found that $La_{10}Al_4O_{21}$ has less reducing ability compared to $LaAlO_3$. The values of H_2 consumption at different peak temperatures are listed in Table III. The higher amount of H_2 consumption shows the higher amount of reactive oxygen in $LaAlO_3$ [28].

Table Iii Quantitative H_2-Tpr Analysis Of Nano Lanthanum Aluminate

Sample	Peak temperature(°C)	H_2 consumption (μmolg^{-1})
$La_{10}Al_4O_{21}$	662.5	180.51
	678.9	136.9
$LaAlO_3$	691.8	297.8
	732.2	135.9

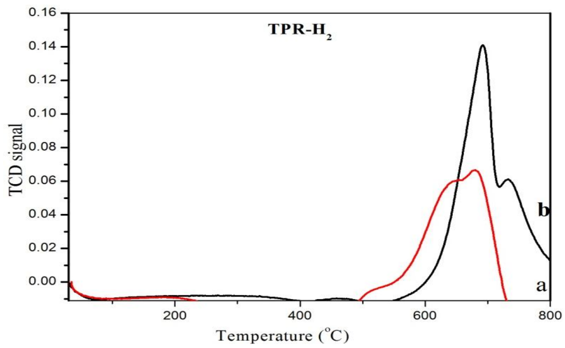

Fig. 8 H_2-TPR profile of nano mesoporous (a) $La_{10}Al_4O_{21}$ (b) $LaAlO_3$

9) Dielectric Properties and ac Conductivity Measurement: The effect of ac frequency on capacitance, loss tangent and dielectric constant at room temperature for lanthanum aluminates are shown in Fig. 9. Dielectric relaxation observed in lanthanum aluminates may be due to the fact that the species contributing to the polarizability are lagging behind the applied field at higher frequency [29]. Higher capacitance and dielectric constant of $LaAlO_3$ may be due to its mesoporous nature and higher interface, orientation, ionic and electronic polarizations compared to $La_{10}Al_4O_{21}$.

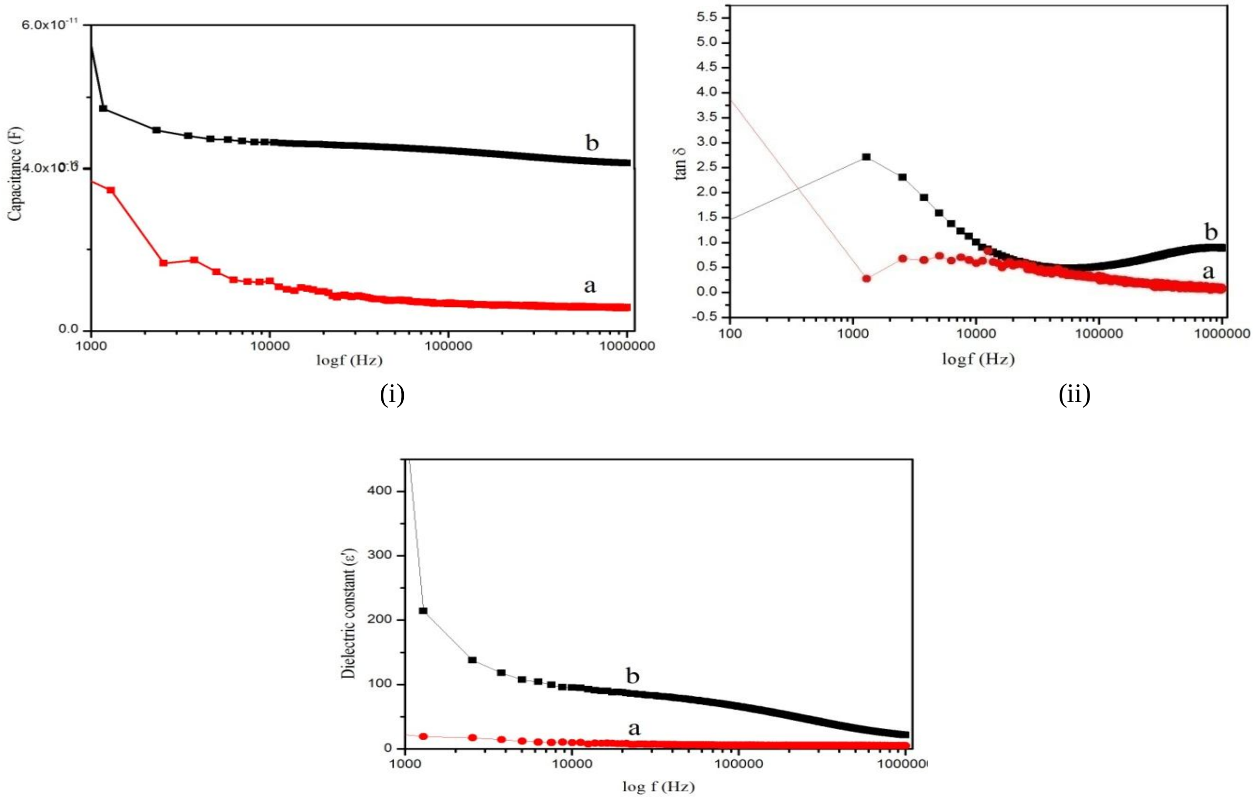

(i)

(ii)

(iii)

Fig. 9 Frequency dependent variation of (i) capacitance, (ii) loss tangent and (iii) dielectric constant of nano (a) $La_{10}Al_4O_{21}$ (b) $LaAlO_3$

To understand the conduction mechanism, the variation of ac conductivity as a function of frequency is measured, Fig. 10. As depicted in the Fig.10, ac conductivity increases with increasing frequency. Low percolation probability and low moisture content of nano mesoporous $LaAlO_3$ may be the reason for its very high ac conductivity compared to nano $La_{10}Al_4O_{21}$[30].

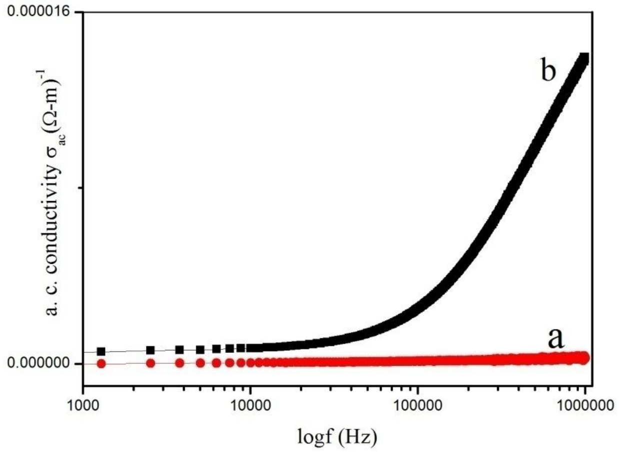

Fig. 10 Frequency dependent variation of ac conductivity in nano (a) $La_{10}Al_4O_{21}$ (b) $LaAlO_3$

B. *Catalytic Reactions*

The FC benzylation of o-Xyl with BC was carried out using stable nano mesoporous $LaAlO_3$ at different reaction temperature, catalyst weight and reaction time for 1:1 and 5:1 molar ratio of o-Xyl/BC and extended to $La_{10}Al_4O_{21}$ at the optimized conditions. Benzylation of o-Xyl was also carried out in the absence of catalyst and no obvious BC conversion was detected

1) *Thermal Analysis:* The effect of catalyst concentration in the range of 0.05-0.25 g mol^{-1} of BC on the conversion of BC is studied at 433 K for 2 h of reaction for different molar ratios of o-Xyl/BC over nano mesoporous $LaAlO_3$ as catalyst. The catalysts to BC ratios are changed by keeping the constant concentration of BC in the reaction mixture. When the catalyst to BC ratio is increased from 0.05 to 0.25, the conversion of BC is also found to increase from 14 to 100 % for 1:1 o-Xyl/BC molar ratio and 40 to 100% for 5:1 o-Xyl/BC molar ratio. A reaction rate plateau appears when the catalyst weight exceeds 0.2 g mol^{-1} of BC for 1:1 o-Xyl/BC molar ratio and 0.25 g mol^{-1} of BC for 1:5 o-Xyl/BC molar ratios. These results confirm that with an increase in catalyst loading the conversion of BC increases because of the increase in the total number of acidic sites available for the reaction [15]. 3,4-Dimethyl Diphenylmethane (3, 4-DMDPM) was detected as the major product.

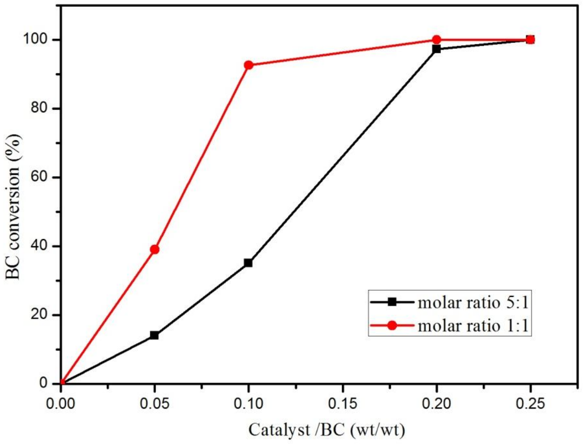

Fig. 11 Effect of catalyst/BC molar ratio on the conversion of BC for different molar ratios of o-Xyl/BC

2) *Effect of Reaction Temperature:* The temperature dependency of this reaction at the following reaction conditions (catalyst to BC (w/w) = 0.1, 2h, 1 atm) for different molar ratios of o-Xyl/BC is shown in Fig. 12. BC conversion over $LaAlO_3$ as catalyst increases steadily from 20 to 100% for 1:1 o-Xyl/BC molar ratio and 1 to 54% for 5:1 o-Xyl/BC molar ratio as the temperature is raised from 302 to 473 K.

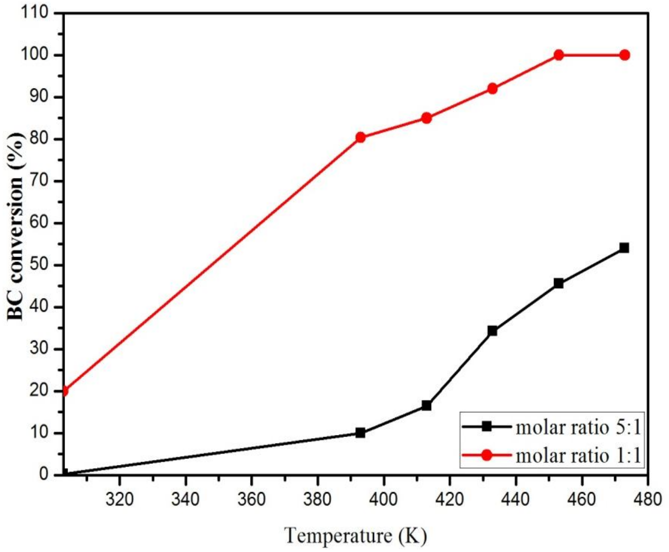

Fig. 12 Effect of reaction temperature on the conversion of BC for different molar ratios of o-Xyl/BC

3) *Effect of reaction Time:* The relationship between conversion of BC and reaction time for benzylation of o-Xyl over $LaAlO_3$ and $La_{10}Al_4O_{21}$ catalysts is illustrated in Fig. 13 at the following reaction conditions (catalyst to BC (w/w) = 0.1, o-Xyl/BC molar ratio =1:1, 433K, 1 atm). $LaAlO_3$ gave higher conversion compared to $La_{10}Al_4O_{21}$. The conversion of BC over $LaAlO_3$ is found to be increased with the increase in the reaction time and reaches a maximum (92%) in 2 h of the run. $La_{10}Al_4O_{21}$ exhibit comparatively lower activity (51%) in this reaction. Large no of acidic sites and mesoporous structure of $LaAlO_3$ may be responsible for higher catalytic activity. The catalytic activity correlated well with their reducing ability, since the variation in the activities seems to follow the change in the reducing ability. This redox property was expected to play an important role for initiating benzyl carbocation ($C_6H_5CH_2^+$) for the reaction [13].

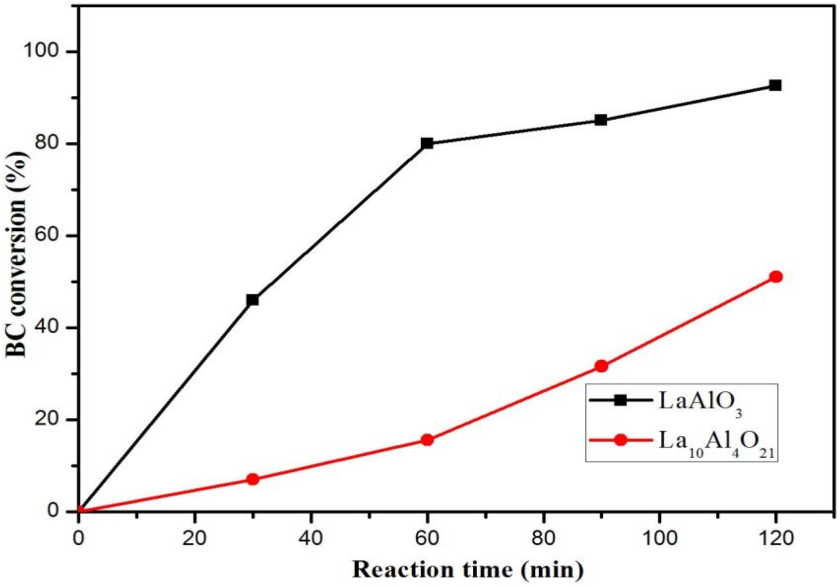

Fig. 13 Reaction time versus BC conversion over lanthanum aluminates

4) *Effect of o-Xyl/BC molar ratio:* Fig.14 shows the effect of varying the o-Xyl/BC molar ratio in the reaction mixture on the activity of nano mesoporous $LaAlO_3$ at a fixed BC concentration at the following reaction conditions (catalyst to BC (w/w) = 0.1, 433K, 1 atm). An increase in the BC conversion is observed with the decrease in o-Xyl/BC molar ratio. The study indicates that using excess o-Xyl results into fast deactivation of active sites, which may be attributed to passivation of active sites by strong adsorption of excessive o-Xyl molecule.

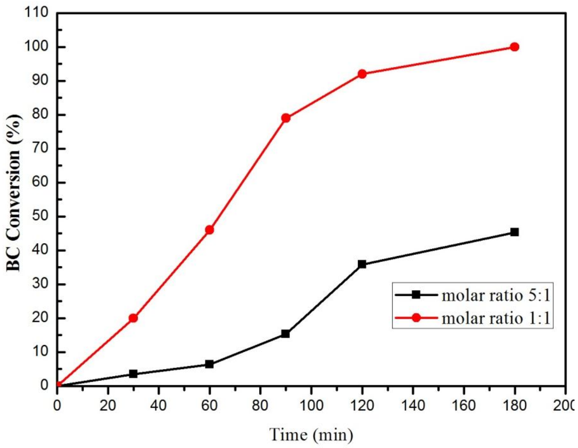

Fig. 14 Effect of o-Xyl/BC molar ratio on the conversion of BC

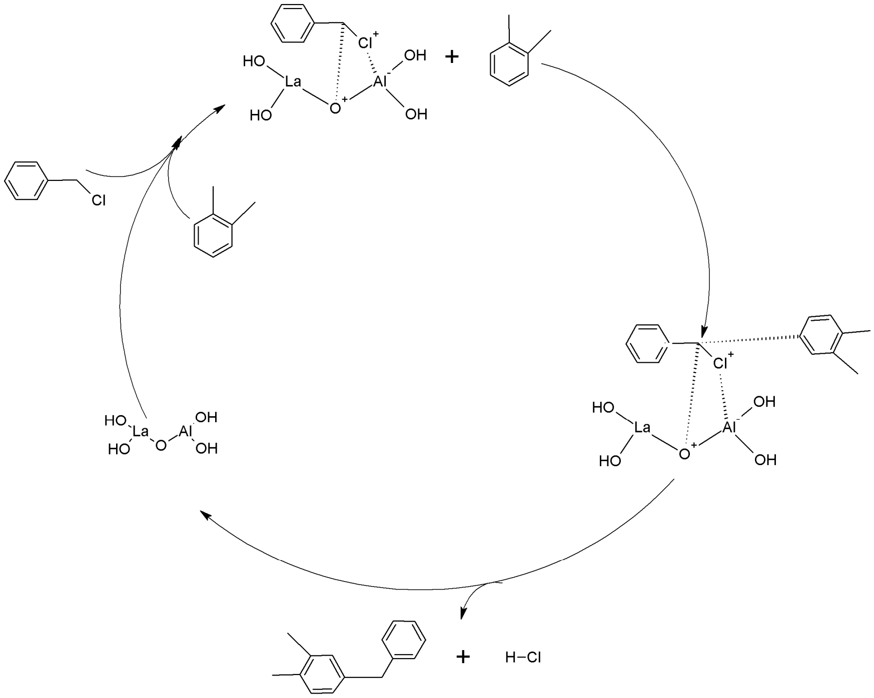

Fig. 15 Proposed reaction mechanism for the benzylation of o-Xyl using lanthanum aluminate catalyst

5) *Proposed Reaction Mechanism*: Generally benzylation of aromatics takes place by electrophilic aromatic substitution. A schematic diagram of the catalytic cycle for the benzylation of o-Xyl using lanthanum aluminate catalyst is represented in Fig. 15. The figure suggests that acidic $LaAlO_3$ polarizes the BC molecule into an electrophile ($C_6H_5CH_2^+$) which then attacks the o-Xyl ring resulting in the formation of 3, 4-DMDPM.

IV. CONCLUSIONS

Sol-gel method is used to prepare nano crystalline lanthanum aluminate powders. $La_{10}Al_4O_{21}$ developed at lower aluminum precursor concentration changes to stable $LaAlO_3$ as concentration increases. XRD and FTIR analysis confirmed the formation of $LaAlO_3$ and $La_{10}Al_4O_{21}$. $La_{10}Al_4O_{21}$ found to have lower particle size and higher surface area compared to $LaAlO_3$. Mesoporous structure of $LaAlO_3$ and macroporous structure of $La_{10}Al_4O_{21}$ was revealed from BJH isotherm. UV-Vis absorption spectrometric data revealed large band gap of $La_{10}Al_4O_{21}$ (5.2 eV) in comparison with $LaAlO_3$ (4.6 eV). CO_2-TPD, NH_3-TPD and H_2-TPR analysis results indicate small basicity, high acidity and high reduction potential of $LaAlO_3$ related to $La_{10}Al_4O_{21}$. $LaAlO_3$ found to have high ac conductivity and large dielectric constant compared to $La_{10}Al_4O_{21}$. Nano mesoporous $LaAlO_3$ was found to be an efficient catalyst compared to nano $La_{10}Al_4O_{21}$ in the benzylation of o-Xyl. $LaAlO_3$ showed 92% BC conversion where as nano $La_{10}Al_4O_{21}$ exhibits 51% BC conversion at the same experimental conditions. The higher activity of $LaAlO_3$ may be attributed to its stronger acidic sites and mesoporous structure. The higher yield of product can be achieved by increasing reaction parameters such as; reaction temperature, catalyst concentration and reaction time, while the conversion is found to decrease with increase in molar ratio of o-Xyl/BC. The formation of 3, 4-DMDPM is explained by an electrophilic attack of the benzyl cation ($C_6H_5CH_2^+$) on the o-Xyl ring whose formation is facilitated by the stronger acid sites of catalyst.

V. ACKNOWLEDGMENT

The authors gratefully acknowledge UGC, New Delhi for pro-viding FIP to one of the authors Marymol Moothedan and also acknowledge the support of the Principal, Mar Athanasius College, Kothamangalam for providing infrastructure facilities. The technical assistance from SAIF, CUSAT were also acknowledged.

REFERENCES

[1] L. Vasylechko, A. Senyshyn, and U. Bismayer, Perovskite-Type Aluminates and Gallates, Handbook on the Physics and Chemistry of Rare Earths, Vol. 39, Netherlands: North-Holland, 2009.

[2] Bin Liu, Feng Yuan, Xiao Hu, “Impurity induced resonance states at the superconducting interface $LaAlO_3$/$SrTiO_3$”, Journal of Physics and Chemistry of Solids, vol. 72, pp.380–383,2011.

[3] V.H. Oliveira, N.M. Khaidukov, E.C. Silva, L.O. Faria, “Study of TL properties of $LaAlO_3$:Ce,Dy crystals for UV dosimetry”, Radiation Measurements, vol.46, pp.1173–1175, 2011.

[4] X.B. Lu, P.F. Lee, J.Y. Dai, “Effects of forming gas annealing on the memory characteristics of Ge nanocrystals embedded in $LaAlO_3$ high-k dielectrics for flash memory device application”, Thin Solid Films, vol.513, pp.182–186, 2006.

[5] X.B. Lu, H.B. Lu, J.Y. Dai, Z.H. Chen, M. He, G.Z. Yang, H.L.W. Chan, C.L. Choy, “Oxygen pressure dependence of physical and electrical properties of $LaAlO_3$ gate dielectric”, Microelectronic Engineering , vol.77, pp. 399–404,2005.

[6] Zahra Negahdari, Monika Willert-Porada, Florian Scherm, “Thermal properties of homogenous lanthanum hexaaluminate/alumina composite ceramics”, Journal of the European Ceramic Society, vol. 30, pp. 3103–3109, 2010.

[7] Xiaoguang Ren, Jiandong Zheng,Yongji Song, Ping Liu, “Catalytic properties of Fe and Mn modified lanthanum hexaaluminates for catalytic combustion of methane”, Catalysis Communications, vol. 9, pp. 07–810, 2008.

[8] Nabanita Pal, Manidipa Paul, Asim Bhaumik, “New mesoporous perovskite ZnTiO3 and its excellent catalytic activity in liquid phase organic transformations”, Applied Catalysis A: General, vol. 393, pp. 153–160, 2011.

[9] N. Alves, W.B. Ferraz, L.O. Faria, “Synthesis and investigation of the luminescent properties of carbon doped lanthanum aluminate ($LaAlO_3$) for application in radiation dosimetry”, Radiation Measurements, vol. 71, pp. 90–94, 2014.

[10] Tomasz Brylewski, Mirosław M. Bućko, “Low-temperature synthesis of lanthanum monoaluminate powders using the co-precipitation–calcination technique”, Ceramics International, vol. 39, pp. 5667–5674, 2013.

[11] Shuai Li, Bill Bergman, Zhe Zhao, “Synthesis and characterization of lanthanum aluminate powders via a polymer complexing plus combustion route”, Materials Chemistry and Physics,vol.132, pp. 309–315, 2012.

[12] Magnus Rueping, Boris J. Nachtsheim, “A review of new developments in the Friedel–Crafts alkylation – From green chemistry to asymmetric catalysis”, Beilstein J. Org. Chem., vol. 6, pp. 1-24, 2010.

[13] Farook Adam, Adil Elhag Ahmed, “The benzylation of xylenes using heterogeneous catalysts from rice husk ash silica modified with gallium, indium and iron,” Chemical Engineering Journal,vol. 145, pp. 328–334, 2008.

[14] Chitralekha Khatri, Manish K. Mishra, Ashu Rani, “Synthesis and characterization of fly ash supported sulfated zirconia catalyst for benzylation reactions”, Fuel Processing Technology, vol. 91, pp. 288–1295, 2010.

[15] Ganapati D. Yadav, Shashikant B. Kamble, “Friedel–Crafts green alkylation of xylenes with tert-butanol over mesoporous superacid UDCaT-5”, Chemical Engineering Research and Design,vol. 90, pp. 1322–1334, 2012.

[16] X.-S. Liu, Jiqing Lu, L.-Y. Jin, M.-F. Luo, “High surface area Ceo.9Cuo.iC>2-5 and Ceo.9Mrio.1O2.5 solid solutions for CO and HCHO oxidation”, Indian J. Chemistry, vol. 48, pp. 1352-1357, 2009.

[17] Y. B. R. D. Rajesh, R. S. Dubey, “Sol-Gel Synthesis and Characterization of Nanocrystalline Spinel LiMn2O4 For Battery Applications”, Nanoscience and Nanoengineering, vol. 1, pp. 139-141, 2013.

[18] Shantanu K. Behera _, Prashant K. Sahu, Swadesh K. Pratihar, Santanu Bhattacharyya, “Phase evolution in gel-precipitated LaAlO3 ceramics”, Journal of Physics and Chemistry of Solids,vol. 69, pp. 2041-2046, 2008.

[19] Yebin Xu, Guohua Huang, Hua Long, “Synthesis of lanthanum aluminate via the ethylenediaminetetraacetic acid gel route”, Ceramics international, vol. 29, pp. 837-840, 2003.

[20] G.C.C. Costa, R. Muccillo, “Synthesis of lanthanum beta-alumina powders by the polymeric precursor technique”, Ceramics International, vol. 34, pp. 1703–1707, 2008.

[21] Chen B, Yu J, Liang X., “LaAlO3 hollow spheres: synthesis and luminescence properties”, Langmuir, vol. 27, pp. 11654-9, 2011.

[22] M. A. Humayun, M. A. Rashid, F. A. Malek, A. N. Hussain, “Effect of lattice constant on band-gap energy and optimization and stabilization of high-temperature $In_xGa_{1-x}N$ quantum-dot lasers”, Journal of Russian Laser Research, vol. 33, pp. 387-394, 2012.

[23] Weilun Wang, Peng Liu, Ming Zhang, Jiashan Hu, Feng Xing, “The Pore Structure of Phosphoaluminate Cement”, Open Journal of Composite Materials, vol. 2, pp. 104-112, 2012.

[24] Ali Sdiri, Teruo Higashi, Samir Bouaziz, Mourad Benzina, “Synthesis and characterization of silica gel from siliceous sands of southern Tunisia”, Arabian Journal of Chemistry, vol. 7, pp. 486–493, 2014.

[25] Yan, J., Yu, D., Sun, P., Huang, H., “Alkaline earth metal modified NaY for lactic acid dehydration to acrylic acid: Effect of basic sites on the catalytic performance original research article”, Chin. J. Catal., vol. 32, pp. 405-411, 2011.

[26] Liguo Wang, Yubo Ma, Ying Wang, et al., “Efficient synthesis of glycerol carbonate from glycerol and urea with lanthanum oxide as a solid base catalyst”, Catalysis Communications., vol. 12, pp. 1458-1462, 2011.

[27] Johannes A. Lercher,Christian Grundling, Gabriele Eder-Mirth, “Infrared Studies of the surface acidity of oxides and zeolites using adsorbed probe molecules”, Catalysis today, vol. 27, pp. 353-376, 1996.

[28] María Haidy Castaño, Rafael Molina and Sonia Moreno, “Oxygen Storage Capacity and Oxygen Mobility of Co-Mn-Mg-Al Mixed Oxides and Their Relation in the VOC Oxidation Reaction”, Catalysts, vol. 5, pp. 905-925, 2015.

[29] Abdul Samee Fawzi, A.D. Sheikh,V.L. Mathe, “Structural, dielectric properties and AC conductivity of $Ni_{(1-x)}Zn_xFe_2O_4$ spinel ferrites”, Journal of Alloys and Compounds, vol. 502, pp. 231–237, 2010.

[30] E. Rodr´ıguez-Castello´n J. Jime´nez-Jime´nez, A. Jime´nez-Lo´pez, P. Maireles-Torres, J.R. Ramos-Barrado , D.J. Jones , J. Rozie`re, “Proton conductivity of mesoporous MCM type of zirconium and titanium phosphates”,Solid State Ionics, vol. 125, pp.407–410,1999.

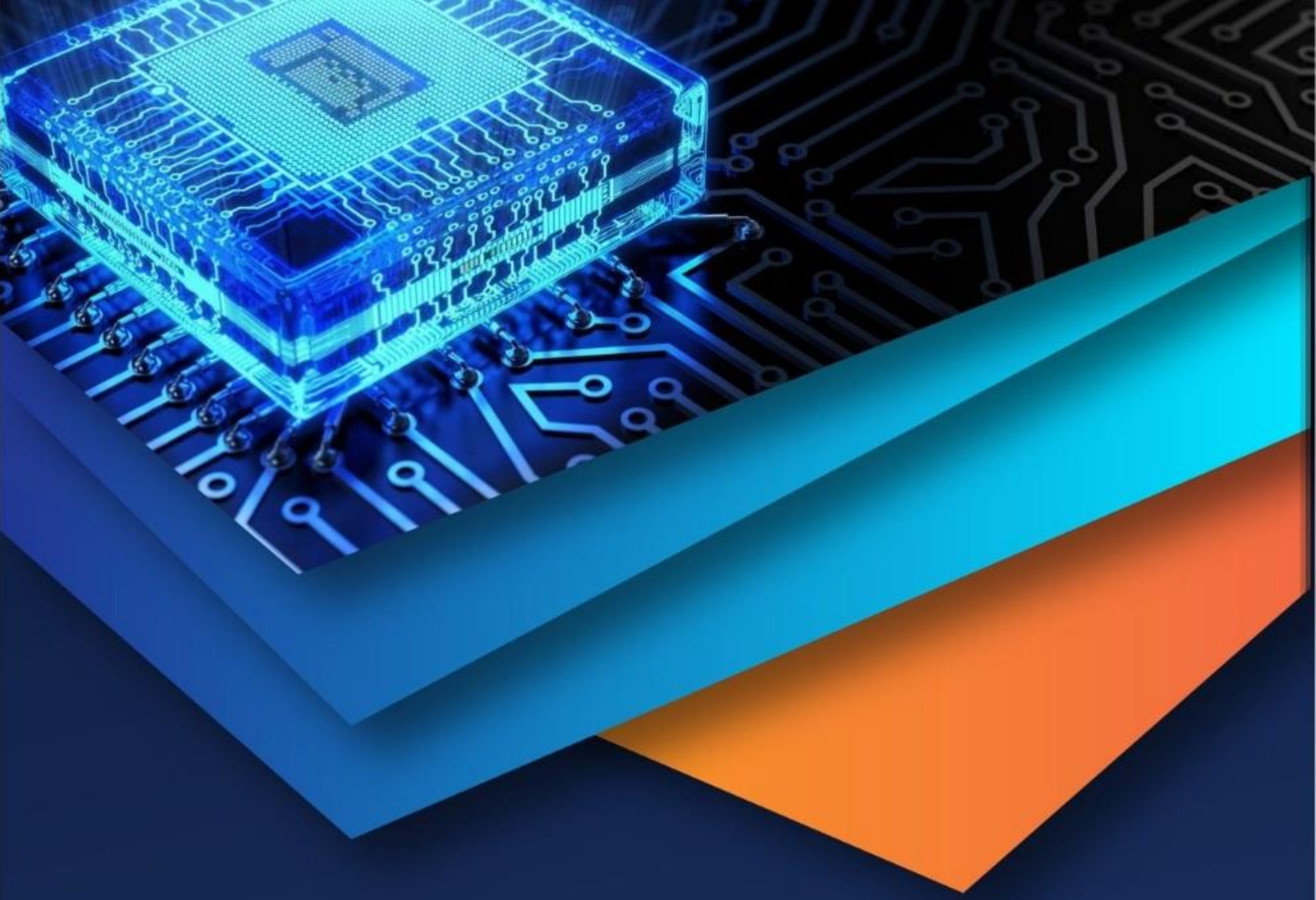

10.22214/IJRASET

INDEX COPERNICUS
45.98

IMPACT FACTOR:
7.129

TOGETHER WE REACH THE GOAL
IMPACT FACTOR:
7.429

INTERNATIONAL JOURNAL FOR RESEARCH

IN APPLIED SCIENCE & ENGINEERING TECHNOLOGY

Call : 08813907089 ✆ (24*7 Support on Whatsapp)